Spin wave stiffness and exchange stiffness of doped permalloy via *ab initio* calculations

O. Šipr,[1,2,*] S. Mankovsky,[3] and H. Ebert[3]

[1]*Institute of Physics of the Czech Academy of Sciences, Cukrovarnická 10, CZ-162 53 Prague, Czech Republic*
[2]*New Technologies Research Centre, University of West Bohemia, CZ-306 14 Pilsen, Czech Republic*
[3]*Universität München, Department Chemie, Butenandtstr. 5-13, D-81377 München, Germany*

The way doping affects the spin wave stiffness and the exchange stiffness of permalloy (Py) is investigated via *ab initio* calculations, using the Korringa-Kohn-Rostoker (KKR) Green function formalism. By considering various types of dopants of different nature (V, Gd, and Pt), we are able to draw general conclusions. To describe the trends of the stiffness with doping it is sufficient to account for the exchange coupling between nearest neighbors. The polarizability of the impurities is not important for the spin wave stiffness. Rather, the decisive factor is the hybridization between the impurity and the host states as reflected by changes in the Bloch spectral function. Our theoretical results agree well with earlier experiments.

I. INTRODUCTION

The modification of the properties of magnetic materials by doping is a promising and intensively studied way to make progress in device technology and spintronics. One of the widely studied materials in this respect is permalloy $Fe_{19}Ni_{81}$. It attracts attention because of its high magnetic permeability but also because of its transport properties, which are characterized by a high and low electrical conductivity in the majority and minority spin channels, respectively.

When studying the spin dynamics of materials, the continuum approximation can be often employed. It assumes that the angle of the magnetization changes slowly over atomic distances so that the spin vectors can be replaced by a continuous function $\boldsymbol{m}(\boldsymbol{r})$. The exchange energy is then [1]

$$E[\boldsymbol{m}] = \int_V d^3\boldsymbol{r} \, A_{\mathrm{ex}} \sum_{c=x,y,z} \left(\frac{\partial \boldsymbol{m}}{\partial c} \right)^2. \qquad (1)$$

Here, the exchange stiffness constant A_{ex} is closely connected to the spin wave stiffness constant D via [1]

$$A_{\mathrm{ex}} = \frac{D M_s}{2g\mu_B}, \qquad (2)$$

where M_s is the saturation magnetization, g is the Landé factor ($g \approx 2$ for metals), and μ_B is the Bohr magneton. The spin wave stiffness constant D is linked to the long wavelength limit of the acoustic mode of magnon dispersion [2],

$$\epsilon(\boldsymbol{q}) = D|\boldsymbol{q}|^2 + \beta|\boldsymbol{q}|^4 + \dots, \qquad (3)$$

where $\epsilon(\boldsymbol{q})$ is the magnon energy and $\boldsymbol{q}$ is the corresponding wave vector. From the application point of view, the exchange stiffness is an important characteristic as it determines— together with the magnetic anisotropy—the domain structure of magnetic materials. In addition, it determines magnetization dynamics in them.

Recent interest in the spin wave and/or exchange stiffness of doped permalloy (Py) has been motivated both by fundamental science and by potential applications. Yin *et al.* [3] studied the magnetic properties of Py doped with noble metals Ag, Pt, and Au and found a good agreement between theoretical and experimental values of A_{ex} for dopant concentrations 10–30%. In another study the effect of doping Py by $4d$ and $5d$ elements on the stiffness was studied theoretically for modest concentrations (5–15%) but corresponding experimental data for comparison are lacking [4]. On the other hand, experimental data are available for Py doped with V, Gd, and Pt with concentrations from 1% to 10% thanks to the works of Lepadatu *et al.* [5,6] and Hrabec *et al.* [7].

Tailoring magnetic properties by alloying and doping is one of the very active fields in materials science. It would be useful to understand better the mechanism how different dopants affect the spin wave and exchange stiffness. In particular, it was suggested that the polarizability of the dopant may be an important factor [3,7]. This should be checked and assessed against other possible factors, such as hybridization between host and dopant states. Another question is whether the trends of the spin wave stiffness D and the exchange stiffness A_{ex} with the composition of an alloy system are always the same. The studies often focus either on one quantity or the other. Given the relation Eq. (2) between D and A_{ex} this may be appropriate but then again it is possible that some dopants will have the same influence on D but different influence on M_s, implying that the trends of D will be similar for these dopants but the trends of A_{ex} will differ. Finally, for practical applications it would be helpful to have a simple model or *ansatz* that would enable a quick estimate of how the stiffness will change upon a particular doping.

To address these questions, we present here results of an *ab initio* study of the spin wave stiffness and the corresponding exchange stiffness for Py doped with V, Gd, and Pt. These dopants have quite different electronic and magnetic properties in many respects. Here, the electronic structure is calculated relying on spin-density functional theory. For

---

*sipr@fzu.cz; http://www.fzu.cz/~sipr

the Gd dopant the open core formalism is employed. The exchange coupling constants are then obtained and the D and A_{ex} constants are evaluated and compared to experiment. The influence of the magnetic properties of the dopants is discussed and analyzed. Moreover, it is shown that the effect of doping on D can be parametrized either in terms of the mean-field critical temperature or in terms of the nearest-neighbor coupling. Densities of states and Bloch spectral functions are evaluated and compared to monitor the hybridization between the host and dopant states.

II. THEORETICAL SCHEME

A. Evaluation of the stiffness constants

We assume that the system can be described by a Heisenberg Hamiltonian

$$H = -\sum_{ij} J_{ij} \hat{\boldsymbol{e}}_i \cdot \hat{\boldsymbol{e}}_j, \tag{4}$$

with $\hat{\boldsymbol{e}}_i$ being a unit vector characterizing the orientation of the magnetic moment for the atom i and J_{ij} being the exchange coupling constant. The spin wave stiffness constant D can then be expressed as a sum [8,9]

$$D = \sum_j \frac{2\mu_B}{3\mu_j} J_{0j} R_{0j}^2, \tag{5}$$

where μ_j is the magnetic moment of atom j and R_{0j} is the corresponding interatomic distance. Equation (5) was originally derived for systems containing atoms of one type only. The sum over the atoms $\sum_j$ converges only conditionally, so an additional damping factor has been introduced which enables evaluation of Eq. (5) by extrapolating the partial results to zero damping [9]. Recently the applicability of Eq. (5) was extended to multicomponent systems [4,10,11]. In our case we are dealing with doped Py so we have atoms of three different types located on lattice sites of an fcc structure. If we label atomic types by α and lattice sites by j, the spin wave stiffness constant D can be evaluated as

$$D = \lim_{\eta \to 0} D(\eta), \tag{6}$$

$$D(\eta) = \sum_\alpha c_\alpha D_\alpha(\eta), \tag{7}$$

$$D_\alpha(\eta) = \sum_j \sum_\beta c_\beta \frac{2\mu_B}{3\sqrt{|\mu_\alpha||\mu_\beta|}} J_{0j}^{(\alpha\beta)} R_{0j}^2 e^{-\eta \frac{R_{0j}}{R_{01}}}, \tag{8}$$

where c_α and μ_α are the concentration and the magnetic moment of atoms of type α, $J_{0j}^{(\alpha\beta)}$ is the pairwise exchange coupling constant if an atom of type α is located at the lattice origin and an atom of type β is located at the lattice site j, R_{0j} is the distance of the site j from the lattice origin, η is the damping parameter, and R_{01} is the nearest-neighbor interatomic distance.

When evaluating the sums in Eqs. (7) and (8), one should keep in mind that the magnetic moments are not all of the same nature. Namely, the moments of the V and Pt atoms do not originate from the atoms themselves but are induced by the neighboring Fe and Ni atoms. Thus, they cannot be treated as independent entities when describing the tilting

of the magnetic moments. This point was recognized in the past, for example, in connection with efforts to describe the temperature dependence of magnetism of compounds such as FePt [12], FeRh [13], or NiMnSb [14]. A thorough discussion and a way to solve the problem by treating the induced moments via the linear response formalism can be found in Ref. [15]. In our case the situation is different because we are interested in the spin wave stiffness for $T = 0$, which is determined by the energetics of spin waves in the long-wavelength limit, where the angles between the spins are very small and the corresponding decrease of the induced magnetic moments will be also very small.

Reckoning all this, we deal with the moments on V and Pt atoms in a hybrid way: We include them in the $\sum_\beta$ sum in Eq. (8) but not in the $\sum_\alpha$ sum in Eq. (7). The V and Pt moments are thus supporting the orientations of magnetic moments at the Fe and Ni atoms but they themselves do not contribute to D directly. To get more insight into the role of the dopant moments, we present further on in Sec. III A also the results obtained when the moments at the dopants were ignored completely in Eqs. (7) and (8) and when they were treated equally as the moments at Fe or Ni atoms, i.e., fully included both in the $\sum_\alpha$ sum in Eq. (7) and in the $\sum_\beta$ sum in Eq. (8). The moments of Gd atoms are intrinsic. Therefore, we treat them in the same way as moments of Fe and Ni atoms, unless explicitly said otherwise.

The exchange stiffness constant A_{ex} was obtained from the spin wave stiffness constant D using Eq. (2). The saturation magnetization M_s was determined as the magnetic moment per unit cell (always including the contributions of all atomic types). The Landé factor was taken as $g = 2.1$ [16,17].

B. Computational method

The calculations were performed within the *ab initio* framework of the spin-density functional theory, relying on the generalized gradient approximation (GGA) using the Perdew, Burke, and Ernzerhof (PBE) functional. The electronic structure was calculated in a scalar-relativistic mode using the spin-polarized multiple-scattering or Korringa-Kohn-Rostoker (KKR) Green function formalism [18] as implemented in the SPRKKR code [19]. For the multipole expansion of the Green function, an angular momentum cutoff $\ell_{max} = 3$ was used. The disorder was treated within the coherent potential approximation (CPA). The potentials were subject to the atomic sphere approximation (ASA). Identical atomic radii were used for all atomic species on a given site, as is common in CPA calculations. By doing this we neglect effects of local lattice relaxations and may effectively introduce some artificial charge transfer [20]. We do not expect that this affects our conclusions significantly. In principle, these constraints could be bypassed by employing unequal constituent atoms radii [21]. For each dopant concentration, the equilibrium lattice constant a_0 was determined by minimizing the total energy. The exchange coupling constants $J_{0j}^{(\alpha\beta)}$ were evaluated from the electronic structure using the prescription of Liechtenstein *et al.* [8].

Taking the limit $\lim_{\eta \to 0} D(\eta)$ in Eq. (6) is a delicate issue. To avoid errors in extrapolating $D(\eta)$ to $\eta = 0$, one should evaluate $D(\eta)$ down to as low η as possible. However, low

η implies that the sum Eq. (8) converges slowly with the distance R_{0j}. One should, therefore, extend the sum $\sum_j$ to large distances. Evaluating the exchange coupling constants $J_{0j}^{(\alpha\beta)}$ for large R_{0j} requires a very dense mesh in the $\mathbf{k}$ space to avoid numerical errors for the structure constants. In our case the situation is not so critical because we are dealing with alloys, meaning that the requirements on the extent of the $\sum_j$ sum in Eq. (8) and on the density of the $\mathbf{k}$ mesh in evaluating the $J_{0j}^{(\alpha\beta)}$ constants are not so demanding. Nevertheless, to be on the safe side, the $\mathbf{k}$-space integration was carried out via sampling on a regular mesh corresponding to $62 \times 62 \times 62$ points in the full Brillouin zone and the $\sum_j$ sum in Eq. (8) covered interatomic distances up to 20.5 a_0 (corresponding to about 136 000 atomic sites). With these settings numerically accurate values of $D(\eta)$ were obtained for η ranging from 0.2 to 1. The extrapolation to $\eta = 0$ was done using a fifth-degree polynomial.

A proper description of magnetism of Gd requires going beyond the GGA. Many aspects of magnetism of rare earth metals can be described within the open-core formalism, where the f electrons are treated as tightly bound core electrons and their number is kept fixed to an integer number during the self-consistency loop [22]. In particular it was shown that the exchange coupling of Gd and its compounds can be described by the open core formalism quite well [23–25]. Therefore we employ it here when discussing the impact of doping by Gd atoms. More specifically, we used a mixed approach where we first calculate the electronic structure of Gd-doped Py via the open core formalism and then we use the self-consistent potential obtained thereby to evaluate the exchange coupling constants in a standard way, i.e., treating the Gd f electrons as valence electrons. To check whether this approach is justified, we compared the density of states (DOS) obtained via both approaches. We found that the positions of the Gd f states practically do not depend on whether they are provided by the open core calculation itself or whether they are derived from the peaks in the density of the Gd f states obtained by a "standard" calculation for the potential generated by the open-core formalism (data not shown). It turns out in the end that use of the open core formalism is not crucial, the stiffness constants obtained in this way are very close to the constants obtained by relying solely on the bandlike description of the f electrons. The equilibrium lattice constant a_0 was evaluated always within the GGA, for all dopant types.

III. RESULTS

A. Comparing calculated values for D and A_{ex} with experiment

Results obtained for the equilibrium lattice constant a_0, magnetization per unit cell M_s, and spin wave stiffness D for V-doped Py are shown in Table I. As discussed in Sec. II A, we show D obtained when treating the moments of the V atoms as supporting, i.e., omitting them in the $\sum_\alpha$ sum in Eq. (7) but keeping them in the $\sum_\beta$ sum in Eq. (8). The magnetic moments of the V atoms are oriented antiparallel to the moments at the Fe and Ni atoms, therefore the magnetization M_s decreases rapidly with increasing concentration of the V atoms.

TABLE I. Equilibrium lattice constant a_0, magnetic moment per unit cell M_s, and spin waves stiffness constant D for V-doped Py.

conc. (%)	a_0 (a.u.)	M_s (μ_B/cell)	D (meV Å^2)
0.0	6.658	1.017	576
1.0	6.662	0.982	534
2.5	6.666	0.926	478
3.5	6.670	0.888	444
6.0	6.676	0.799	369
10.0	6.695	0.671	273

Analogous results for Gd-doped Py are shown in Table II. We present here D calculated by three different methods: (i) ignoring the moments at Gd atoms altogether [omitting them both in the $\sum_\alpha$ sum and in the $\sum_\beta$ sum in Eqs. (7) and (8)], (ii) treating them as supporting [omitting them in the $\sum_\alpha$ sum in Eq. (7) but keeping them in the $\sum_\beta$ sum in Eq. (8)], and (iii) treating the Gd moments equally as the Fe and Ni moments (including them in the $\sum_\alpha$ sum and in the $\sum_\beta$ sum). It is obvious from Table II that the way the Gd moments are treated does not really matter for the spin wave stiffness of Gd-doped Py.

The influence of using the open core formalism for Gd-doped Py is shown in Table III. It contains the magnetization M_s and the spin wave stiffness D calculated for the potential obtained using the open core formalism and for the potential obtained via the GGA. One can see that the difference between both procedures is not significant in this regard.

Results for Pt-doped Py are shown in Table IV. Here we show additionally the experimental results for D at zero temperature obtained by Yin *et al.* [26]. The experimentally observed decrease of D with increasing Pt concentration is similar to the decrease obtained by theory.

Our focus is on comparing the trends of D and A_{ex} with the dopant concentration for different dopant types. This is inspected in Fig. 1. One can see that the spin wave stiffness D for V-doped Py and Gd-doped Py is practically the same. The difference appears only for the exchange stiffness A_{ex} and stems from the differences in the magnetization for these two systems (cf. the third columns of Tables I and II). The experimental data are shown in the bottom graph of Fig. 1. Both experiment and theory suggest that the decrease of the exchange stiffness A_{ex} with increasing dopant concentration

TABLE II. Equilibrium lattice constant a_0, magnetic moment per unit cell M_s, and spin waves stiffness constant D for Gd-doped Py. The unit for D is meV Å^2.

conc. (%)	a_0 (a.u.)	M_s (μ_B/cell)	dopants ignored	dopants supporting	dopants as equal
				stiffness constant D	
0.0	6.658	1.017	576	576	576
1.0	6.693	1.067	531	531	530
5.0	6.803	1.244	380	381	381
10.0	6.952	1.477	242	243	243

TABLE III. Magnetic moments per unit cell M_s and spin waves stiffness constant D for Gd-doped Py obtained by taking the potential from the open-core calculations and from the GGA-based band structure calculations.

conc.	open-core potential		GGA potential	
	M_s	D	M_s	D
(%)	(μ_B/cell)	(meV $\mathring{A}^2$)	(μ_B/cell)	(meV $\mathring{A}^2$)
1.0	1.067	531	1.066	532
5.0	1.244	381	1.239	387
10.0	1.477	243	1.463	250

is approximately linear and that this decrease is quickest for the V dopant and slowest for the Pt dopant.

Concerning the absolute values of A_{ex}, part of the difference between theory and experiment is due to the temperature effects. The theoretical data are for zero temperature. The experimental data were obtained by fitting the temperature dependence of the magnetization to the Bloch law while assuming implicitly that the stiffness itself does not depend on temperature [5–7]. This is, however, not the case [26–29] meaning that the experimental values for A_{ex} in Fig. 1 correspond to an unknown *effective* temperature. Presumably the effect of this will not be very large: Temperature-dependent measurements of the spin wave stiffness of doped Py indicate that at room temperature the constant D decreases to about 90 % of its zero-temperature value [26]. Therefore we assume that most of the difference in the absolute values of A_{ex} as given by theory and by experiment comes from the spin wave stiffness constant D. Further comments are given at the beginning of Sec. IV below.

One of the intensively studied fundamental questions in connection with the spin dynamics of doped ferromagnets has been about the role of the magnetism of dopant atoms on the exchange and spin wave stiffness [3,7]. We have shown already that the difference in the exchange stiffness A_{ex} between V-doped and Gd-doped Py is because of the difference in the magnetization of these systems, which in turn stems from different magnetic moments at Gd and V

TABLE IV. Equilibrium lattice constant a_0, magnetic moment per unit cell M_s, and spin waves stiffness constant D calculated for Pt-doped Py. Experimental values for D of Yin *et al.* [26] are shown in the last column.

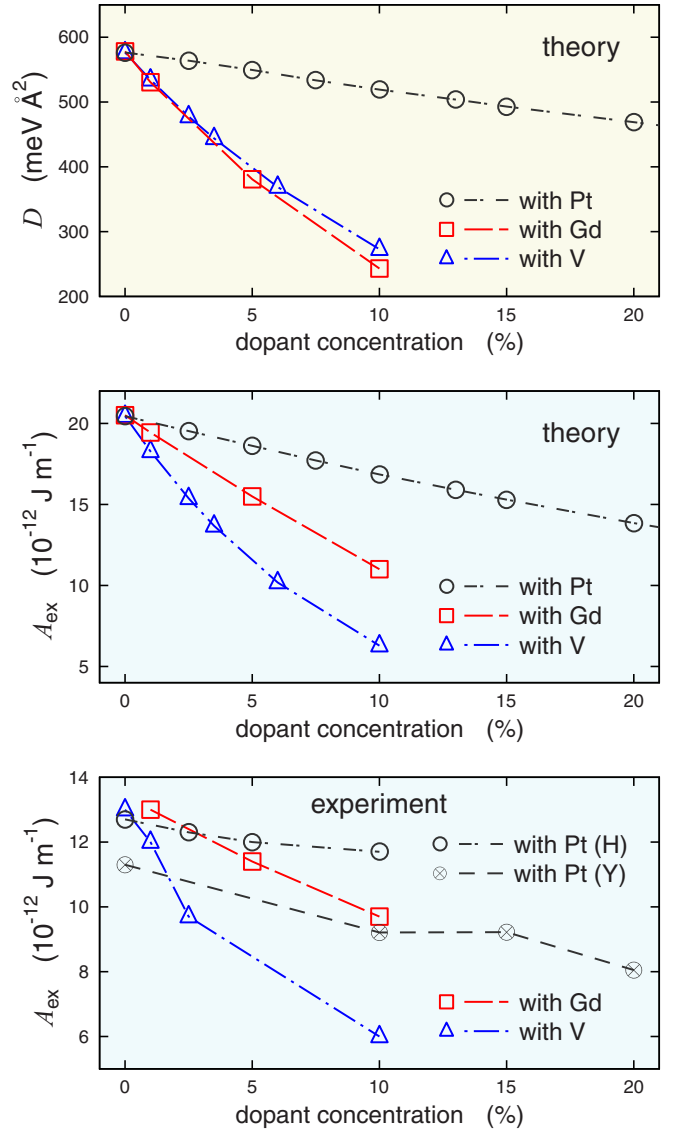| conc.	a_0	M_s	D calc.	D exper.
(%)	(a.u.)	(μ_B/cell)	(meV $\mathring{A}^2$)	(meV $\mathring{A}^2$)
0.0	6.658	1.017	576	442
2.5	6.708	1.015	564	
5.0	6.755	1.014	549	
7.5	6.798	1.013	533	
10.0	6.837	1.007	519	
13.0	6.876	0.997	504	
15.0	6.905	0.992	493	388
20.0	6.972	0.972	469	
30.0	7.078	0.923	420	329

FIG. 1. Theoretical spin wave stiffness D (upper panel) and exchange stiffness A_{ex} (central panel) for Py doped with V, Gd, and Pt. Experimental values for A_{ex} are shown in the lowermost panel, with the data from Ref. [5] for V-doped Py, from Ref. [6] for Gd-doped Py, and from Ref. [7] (circles) and Ref. [3] (circles with crosses) for Pt-doped Py.

atoms. We have also shown that for Gd doping it does not matter for D whether the Gd moments are included in Eqs. (7) and (8) or not (Table II). Let us now turn to the spin wave stiffness for Py doped with V and Pt, both of which are easy to polarize, and compare D evaluated via two extreme approaches: (i) by treating the dopants equally as the host atoms concerning the coupling, i.e., both sums $\sum_\alpha$ in Eq. (7) and $\sum_\beta$ in Eq. (8) include also the dopant atoms, and (ii) by ignoring the coupling for the dopants altogether, i.e., neither of the sums $\sum_\alpha$ and $\sum_\beta$ includes the dopants. The difference between both approaches can be seen in Fig. 2, where we display the results for Pt- and V-doping only; the data for Gd-doped Py are very similar to V-doped Py (cf. the upper panel of Fig. 1). One can see that even though ignoring the coupling for the dopants decreases the values of D by up to
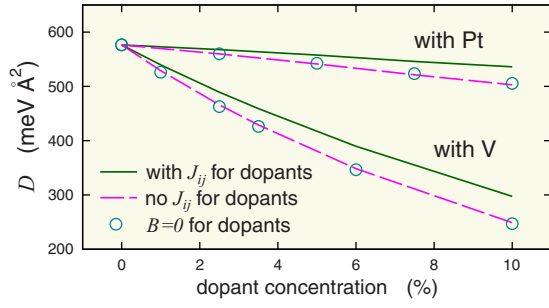
FIG. 2. Spin wave stiffness D for Py doped with V and Pt calculated by considering the coupling constants $J_{ij}^{(\alpha\beta)}$ in Eqs. (7) and (8) for all atoms on the same footing (full lines), by completely ignoring the coupling constants for the dopants (dashed lines), and by additionally suppressing the exchange field B for the dopant atoms (circles).
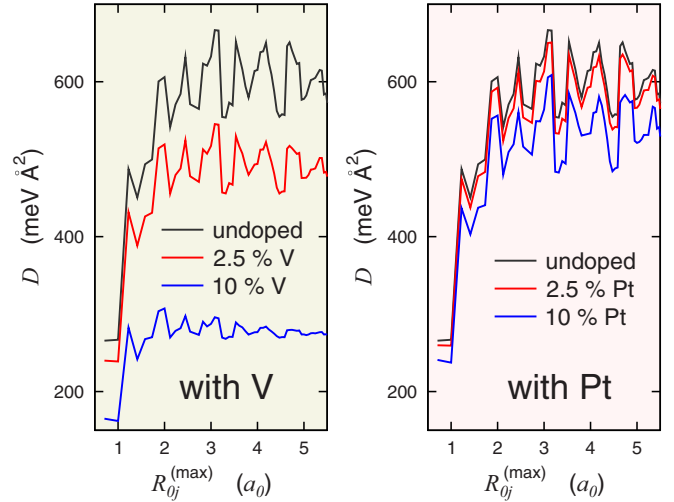

FIG. 3. Dependence of the stiffness constant D on the maximum distance $R_{0j}^{(max)}$ accounted for when evaluating Eq. (8) for undoped permalloy and for permalloy doped by 2.5% and 10% of V (left) and Pt (right).

20% (depending on the concentration), the overall trend and especially the difference between the effect of both dopants does not change. To proceed further, we performed another calculation where the effective local exchange field B was suppressed for the Pt and V dopants. The results (depicted by the circles in Fig. 2) are nearly identical to the situation when the exchange coupling involving the dopant atoms is ignored.

We conclude from this that the polarizability of the dopants does not have a significant influence on the spin wave stiffness D of doped permalloy. The reason why different dopants lead to different results for D must be elsewhere, presumably in the details of the electronic structure and the related hybridization (see Sec. III C below).

B. Influence of dopants on the exchange coupling

In the following we consider the mechanism through which different dopants affect the stiffness of permalloy. The first information concerns the size of the region which effectively determines the spin wave stiffness constant D. We mentioned already that to get good numerical stability, the sum over the sites $\sum_j$ in Eq. (8) has to include sites at very large distances R_{0j} [9]. For a deeper insight, the dependence of the stiffness constant D on the maximum distance $R_{0j}^{(max)}$ up to which the sum $\sum_j$ in Eq. (8) extends is presented in Fig. 3. No damping has been considered for simplicity ($\eta = 0$). The constant D oscillates with $R_{0j}^{(max)}$ and the amplitude of these oscillations decays very slowly. This is why the sum in Eq. (8) has to cover large distances R_{0j} and why the damping factor η has been introduced [9].

It is evident from Fig. 3 that significant variations of the spin wave stiffness constant D only occur within a few nearest shells—up to about $2a_0$ (a_0 is the lattice constant). Afterwards, D just oscillates around the mean value. If the difference in D for two dopant concentrations is big for large $R_{0j}^{(max)}$, it is big also for small $R_{0j}^{(max)}$ and *vice versa*. The difference between V and Pt concerning the rate how D decreases with increasing dopant concentration (see Fig. 1) is evident for small values of $R_{0j}^{(max)}$ already. Including large distances R_{0j} when evaluating Eq. (8) is thus necessary just for technical reasons—to ensure the numerical stability.

Further information about how the nearest neighborhood affects the spin wave stiffness comes from the exchange coupling constants. Figure 4 shows them for the (Fe-Fe), (Fe-Ni), and (Ni-Ni) pairs if they form the nearest neighbors and
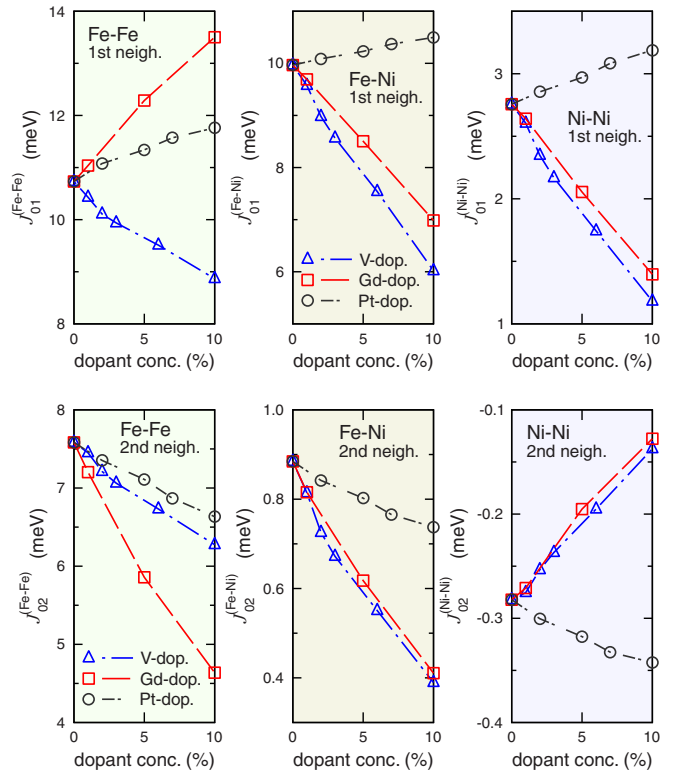

FIG. 4. Exchange coupling constants for Fe-Fe, Fe-Ni, and Ni-Ni atomic pairs if they are first nearest neighbors (upper panels) or second nearest neighbors (lower panels). Data for V-doped Py are shown by triangles, for Gd-doped Py by squares, and for Pt-doped Py by circles.

the next-nearest neighbors. Even though the stiffness constant D has to be evaluated including also pairs whose members are much further apart, the main feature can be seen from J_{01} and J_{02} already: For the (Fe-Ni) and (Ni-Ni) pairs, the coupling constants for V-doped and Gd-doped Py are very similar whereas for Pt-doped Py they differ. As Ni has by far the highest concentration in our systems, this explains why the spin wave stiffness constant D is similar for the V and Gd dopants and different for the Pt dopant.

Based on this, one can speculate that even though a formal evaluation of D requires performing the sum $\sum_j$ in Eq. (8) up to a large distance $R_{0j}^{(\max)}$, the *bare influence of the doping* might be accounted for by a more simple quantity. Let us first focus on the effective total coupling J_0 defined as

$$J_0 = \sum_j J_{0j}, \qquad (9)$$

or, more specifically for our alloy system [cf. Eqs. (7) and (8)],

$$J_0 = \sum_\alpha c_\alpha \sum_j \sum_\beta c_\beta J_{0j}^{(\alpha\beta)}. \qquad (10)$$

This quantity is related to the mean-field Curie temperature via

$$T_C^{(\mathrm{MFA})} = \frac{2}{3} \frac{1}{k_\mathrm{B}} J_0. $$

Note that for a translationally-periodic system, one does not need to perform the $\sum_j$ sum in Eq. (10) explicitly, the J_0 constant can be evaluated from the scattering paths operators in a similar way as the individual J_{ij} constants [8].

The spin wave stiffness constant D is plotted as a function of the effective total coupling J_0 (or, equivalently, $T_C^{(\mathrm{MFA})}$) in the upper left panel of Fig. 5. One can see that for Py doped with various impurities of different concentrations the dependence of D on J_0 is nearly linear. Quantitatively it can be described by

$$D = 79.6 J_0 - 95 \qquad (11)$$

if J_0 is in meV and D in meV Å^2. Using this universal fit, we can recover the dependence of D on the concentration of the impurities by first evaluating J_0 for each system and then getting appropriate D via Eq. (11). The outcome is shown in the lower left panel of Fig. 5. One can see that this model correctly separates the trends for the Pt impurity on one side and for the V and Gd impurities on the other side and that the slope of the dependency of D on the concentration is also reproduced quite well.

To simplify matters even more, one can ask whether the influence of impurities could be possibly described just by focusing on the nearest neighbors. Therefore we inspect the dependence of the stiffness constant D on the effective coupling originating from the nearest neighbors only,

$$J_1 = \sum_\alpha c_\alpha \, 12 \sum_\beta c_\beta J_{01}^{(\alpha\beta)}. \qquad (12)$$

The constant $J_{01}^{(\alpha\beta)}$ characterizes the exchange coupling between the central atom of type α and an atom of type β in the first coordination shell and the factor 12 stands for the number of nearest neighbor sites for the fcc lattice. The resulting
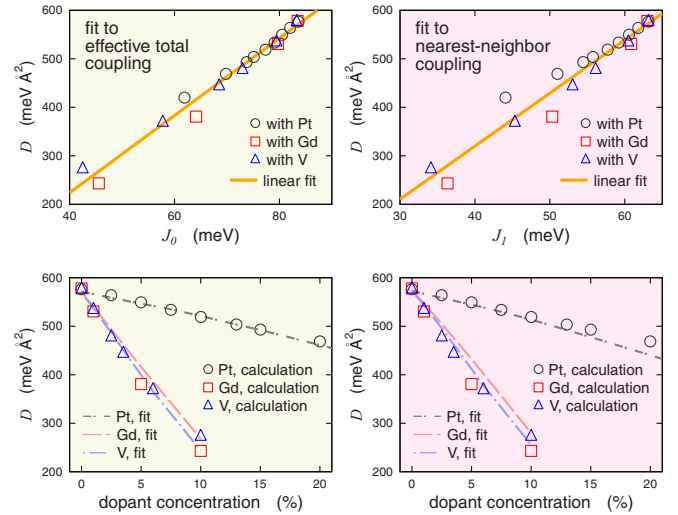

FIG. 5. Upper panels: Dependence of the theoretical spin wave stiffness D on the effective exchange coupling parameter J_0 (left) and on the nearest-neighbor coupling J_1 (right). The markers denote calculated values of D, J_0, and J_1 for different dopants and concentrations, the straight lines show the linear fits. Lower panels: Calculated spin wave stiffness D (markers) together with D obtained from respective J_0 values relying on the linear $D(J_0)$ fit (left) and from respective J_1 values relying on the $D(J_1)$ fit (right).

dependence of D on J_1 is shown in the upper right panel of Fig. 5. The spread around the linear fit

$$D = 109.4 J_1 - 118 \qquad (13)$$

is now bigger than in the case of the $D(J_0)$ dependence but still quite small. Indeed, by relying on Eq. (13), one can get the dependence of D on the impurity concentration with a similar accuracy as by relying on Eq. (11)—compare the lower right panel of Fig. 5 with the lower left panel of the same figure. One could thus say that the *trend* of the spin wave stiffness with the dopant concentration is, to a decisive degree, determined by the coupling between the nearest neighbors. As concerns the *value* of the stiffness constant D, it depends on the interaction within few nearest shells—see Fig. 3 and the related text at the beginning of Sec. III B.

C. Influence of dopants on the electronic structure

The next step is to inspect the electronic structure. The changes in the DOS for the Fe and Ni atoms caused by the doping can be seen in Fig. 6, where we show in the same graphs the data for undoped Py and for Py doped by 10% of V, Gd, and Pt. For the V dopant the changes are minimal: The corresponding DOS curves are hardly distinguishable from each other. For the Pt dopant, the changes are more significant. Still larger but as a whole similar changes can be observed also for the Gd dopant. Based on Fig. 6, one would infer that the hybridization between the electronic states of the host and of the dopant is largest for the Gd dopant and smallest for the V dopant.

Reckoning the results discussed so far, there seems to be a difference in the picture offered by inspecting the J_{ij} constants in Fig. 4 and by inspecting the DOS in Fig. 6. The
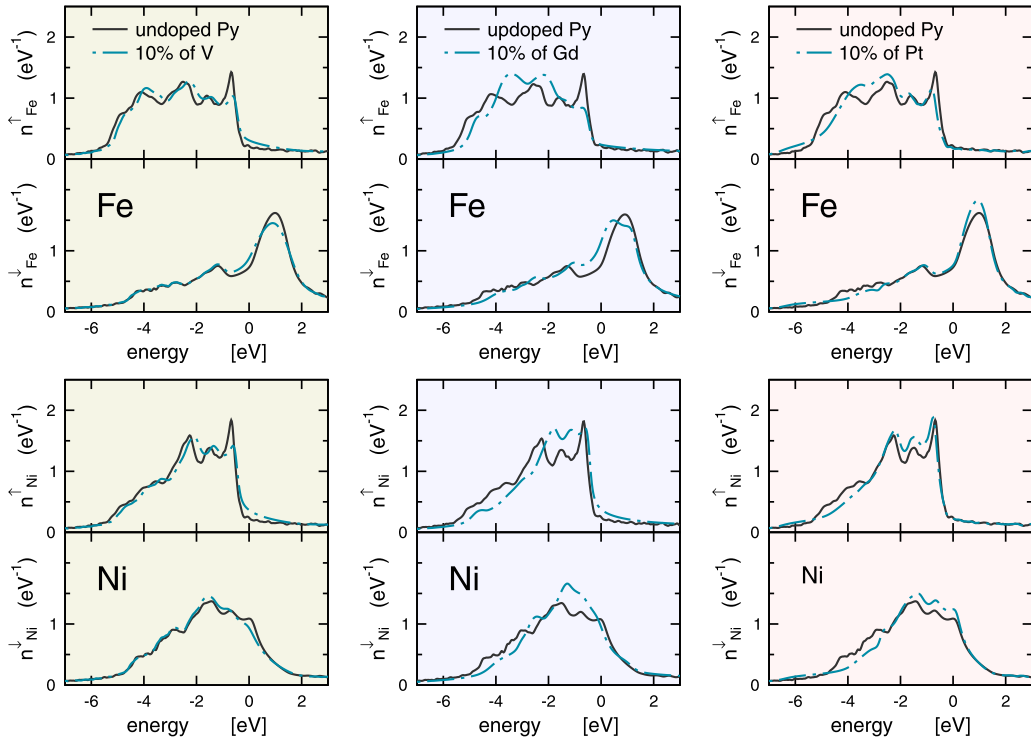
FIG. 6. Upper panels: Comparison of the DOS for Fe atoms in undoped Py and in Py doped by 10% of V (left), Gd (center), and Pt (right). Lower panels: As in the upper panels but for Ni atoms.

analysis of the coupling constants suggests that the V and Gd dopants have a similar effect on the electronic structure (which determines the J_{ij}'s) whereas the influence of the Pt dopant is different. This follows also from spin wave stiffness D shown in Fig. 1. On the other hand, the analysis of the DOS suggests that qualitatively similar effects should follow from introducing the Gd and Pt dopants whereas it is the V dopant which differs in its effect on the electronic structure of permalloy.

A more thorough view on the electronic structure of alloys is provided by the Bloch spectral function $A(\mathbf{k}, E)$, which can be viewed as a $\mathbf{k}$-resolved DOS. The effect of introducing 10% of V, Gd, and Pt into Py is shown in Fig. 7. Left panels show $A(\mathbf{k}, E)$ when the $\mathbf{k}$ vector is varied along straight lines connecting high-symmetry points in the first Brillouin zone, right panels show the Bloch spectral function at the Fermi level $A(\mathbf{k}, E_F)$ when the $\mathbf{k}$ vector spans a two-dimensional section of the $\mathbf{k}$ space (keeping $k_z = 0$). By observing the $E - \mathbf{k}$ scans, one cannot say unambiguously which dopant introduces largest changes to the electronic structure of permalloy. E.g., around the Γ point the smallest changes to $A(\mathbf{k}, E)$ are for the Pt dopant while changes introduced by V or Gd doping are larger. On the other hand, if one focuses on the region around the N point, doping by Gd has the largest impact whereas by V the smallest impact. However, when discussing the spin wave stiffness, one has to keep in mind that it is associated with changes of electron energy caused by spin wave excitations characterized by small wave vector $\mathbf{q}$ and therefore contributed mainly by the electronic states close to the Fermi level E_F. As a result, the spin wave stiffness is sensitive first of all to the electronic structure around E_F. The impact of doping on the states around E_F is illustrated in

the right panels of Fig. 7. Here one can see that the changes introduced by doping by Pt are significantly smaller than changes introduced by doping by V or Gd.

The influence of the doping on the electronic structure around E_F can be quantified by integrating the difference of Bloch spectral functions for a doped system and for an undoped system. We evaluated the integral

$$\int d\mathbf{k} \left| A_X(\mathbf{k}, E_F) - A_{\text{undoped}}(\mathbf{k}, E_F) \right|, \qquad (14)$$

where $A_X(\mathbf{k}, E_F)$ and $A_{\text{undoped}}(\mathbf{k}, E_F)$ are the Bloch spectral functions for doped and undoped systems, respectively, and the integration is carried along the path X-Δ-Γ-Λ-L-Q-W-N-K-Σ-Γ outlined at the horizontal axes of the left graphs in Fig. 7. The results are shown in Table V for two dopant concentrations. The largest changes in the electronic structure are introduced by Gd doping followed by still considerable changes introduced by V doping, while the changes introduced by Pt are small.

TABLE V. Integrals of the differences of Bloch spectral functions at E_F for doped and undoped systems, as defined in Eq. (14). The units are arbitrary.

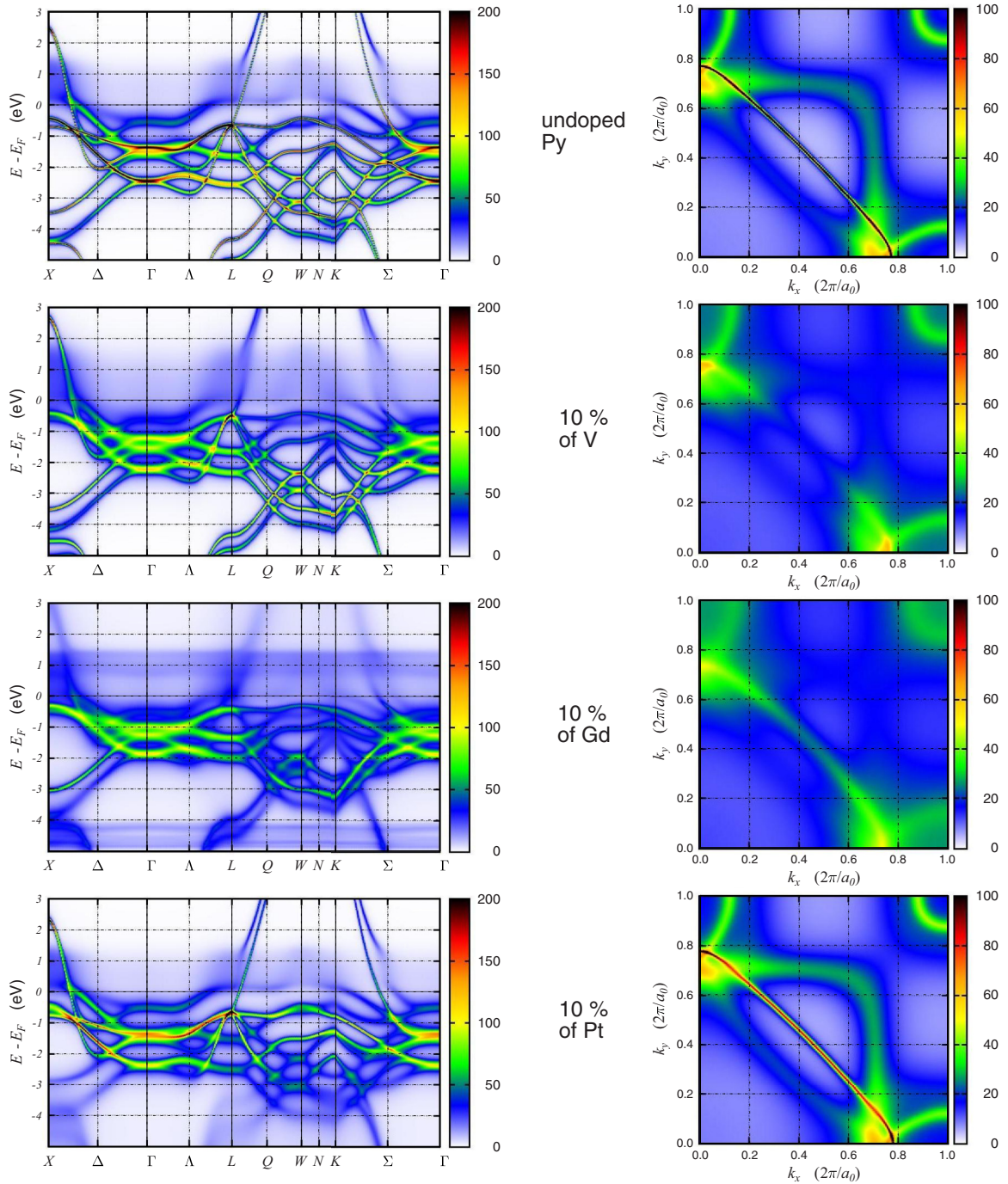| dopant type	concentration 1%	concentration 10%
V	4.49	20.18
Gd	6.07	26.52
Pt	1.38	7.62

FIG. 7. Comparison of Bloch spectral functions for undoped Py and for Py doped by 10% of V, Gd, and Pt.

The picture emerging from analyzing Bloch spectra function is thus different from the picture offered by the DOS. The smallest changes in $A(\mathbf{k}, E)$ with respect to undoped Py are clearly for the Pt dopant. The changes introduced by V or Gd doping are bigger. Based on Fig. 7 and Table V one would assess that the changes in the electronic structure introduced by doping Py with Pt are significantly smaller than the changes introduced by doping Py with V or Gd. Intuitively, this implies that for the Pt dopant the changes in the values of D will be smaller than for the V or Gd dopants—in agreement with the results presented in Sec. III A. The Bloch

spectral function thus offers a more reliable picture than the DOS.

IV. DISCUSSION

Ab initio calculations reproduce the experiment both as concerns the dependence of A_{ex} on the chemical type of the dopant and as concerns the dependence of A_{ex} on the dopant concentration. Regarding the absolute numbers, there are some differences, both between our theory and experiment and between our theory and earlier calculations. In particular

our value of the spin wave stiffness D for undoped permalloy $Fe_{19}Ni_{81}$ of 576 meV Å^2 is higher than 515 meV Å^2 obtained by Yu *et al.* [30] via the tight-binding linear muffin-tin orbital method or 522 meV Å^2 obtained by Pan *et al.* [4] via the KKR-Green's function method. The reason for this is unclear, let us just note that several convergence issues have to be addressed when evaluating D; our settings are given in Sec. II B. Recent experimental values for D of Py are 390 meV Å^2 [31] and 440 meV Å^2 [26], i.e., less than the theoretical values. This is probably linked to problems with describing the exchange coupling of Ni in terms of the coupling constants J_{ij}—there is an even larger difference between theory and experiment for D of fcc Ni [9,30]. Besides, the difference between our values for A_{ex} and the experiment is probably affected also by the temperature dependence of D, which affects the interpretation of some experiments (as mentioned in Sec. III A). Another factor not accounted for by our calculations and possibly affecting the comparison between theory and experiment is the polycrystallinity of the experimental samples that were prepared by sputtering [3,5–7]. One should acknowledge that there may be problems also at the experimental side as the spread of values available in the literature is quite large. A critical assessment would require a standalone study. We just note for illustration that, e.g., in the case of Fe the available experimental data for D include 270 meV Å^2 [32] as well as 307 meV Å^2 [33], in the case of Ni 398 meV Å^2 [34] as well as 530 meV Å^2 [31], and in the case of Py 335 meV Å^2 [35] as well as 390 meV Å^2 [31]. The differences between experimental values of A_{ex} for Pt-doped permalloy reported by Hrabec *et al.* [7] and by Yin *et al.* [3] (cf. Fig. 1) are thus not unusual. Let us summarize that discrepancies between theory and experiment are often observed for the spin wave and/or exchange stiffness and, so far, they are not fully understood.

The fact that the spin wave stiffness D and the exchange stiffness A_{ex} are related through magnetization [see Eq. (2)] which itself is affected by the doping means that there may be situations where doping by two different materials will lead to a similar D but a different A_{ex} (or vice versa). In particular we found that the spin wave stiffness D for V-doped Py and Gd-doped Py is very similar but there is a difference in the exchange stiffness A_{ex} which arises just from the difference in the magnetization (cf. Fig. 1).

The influence of doping on the stiffness D can be discussed just by considering the influence of the atoms in the first coordination shell (Fig. 5). This might appear as surprising reckoning the slow convergence of the sums in Eqs. (5) or (8) [9]. The explanation might be that what we investigate in Fig. 5 is just the *variation of D* with the doping. Equation (13), which we used for our analysis, was derived by fitting the $D(J_1)$ dependence relying on the values of D evaluated by extending the $\sum_j$ sum to the interatomic distance as large as $20.5\,a_0$. However, once the fit according to Eq. (13) has been established, one can predict how the doping will influence the stiffness D just by considering the nearest-neighbors coupling. Our fit has been verified for three quite different dopants so presumably it can be used to assess the effect of doping by other elements as well. This can be helpful in current efforts to manipulate spin-driven properties of materials.

Our results indicate that it does not really matter whether the exchange coupling between the host atoms and the dopant atoms is included in the stiffness calculation or not; the values of D are by about 5% smaller in the latter case but the trends are very similar (see Table II and Fig. 2). This indicates that neither the polarizability of the dopant nor the exchange coupling between the dopant atoms and the host atoms are decisive factors for the spin wave stiffness D (unlike what was conjectured before, see for example Refs. [3,7]). The hybridization between the host states and the dopant states (or lack of it) is more important than the dopant polarizability. Interestingly, this hybridization has to be assessed not from the DOS—which contains only a limited information—but from the Bloch spectral function (cf. Figs. 6 and 7). The fact that inspecting the Bloch spectra function provides a better insight than inspecting the DOS alone can be seen as a demonstration that the exchange coupling constants J_{ij} reflect the full electronic structure, including its **k** dependence.

Earlier studies indicated that the exchange coupling in $4f$-electron systems cannot be properly described within the local density approximation or the GGA. Employing the open core formalism was suggested and tested for this purpose [23]. In our case we found, nevertheless, that the stiffness of Gd-doped Py calculated within the open-core formalism and within the GGA is very similar. The reason for this might be that as the Gd atoms are here just impurities, their f electrons are localized "naturally," by the lack of their hybridization with the host states. A further reduction of the hybridization of the Gd f states via the open core formalism is thus not needed.

Like most other calculations of the spin wave and exchange stiffness we rely on the ASA [2–4,9]. For close-packed metallic systems such as those we are studying here this is not a serious limitation. This was demonstrated, e.g., on a study of magnetic properties of disordered FePt where the CPA was applied both within the ASA and within a full-potential scheme [36].

V. CONCLUSIONS

Ab initio calculations for doped permalloy indicate that the exchange stiffness constant A_{ex} decreases with increasing dopant concentration. This decrease is most rapid for the V dopant followed by the Gd dopant, the slowest decrease is for the Pt dopant—in agreement with experiment. The influence of the V doping and the Gd doping on the spin wave stiffness D is very similar; the difference in the influence of the doping on the exchange stiffness A_{ex} comes from the differences in the magnetization M_s for V-doped and Gd-doped Py. The rate of change of the spin wave stiffness upon introducing the dopants can be discussed by just considering the influence of the atoms in the first coordination shell. The hybridization between impurity and host states is more important for the stiffness than the polarizability of the impurity.

ACKNOWLEDGMENTS

APPENDIX: ACCURACY OF $\lim_{\eta \to 0} D(\eta)$ EXTRAPOLATION

The values of the spin wave stiffness D presented in this paper rely on extrapolating data evaluated according to Eqs. (7) and (8) for finite values of the damping parameter η down to $\eta = 0$. This may be a tricky procedure. To present an analysis of all its aspects would be beyond the scope of this paper but the accuracy of our data can be illustrated on the case of undoped Py. Figure 8 displays original $D(\eta)$ data points together with the fifth-degree polynomial used for the $\eta \to 0$ extrapolation. The D constant obtained without any damping ($\eta = 0$) is shown as well. The error bars depict errors caused by not yet fully damped $D(R)$ oscillations; they are discernible only for $\eta > 0.1$ at this scale. The extrapolating polynomial was found by a least-squares fit within the interval $\eta \in [0.15; 1.00]$. One can see that the fit describes very well also the data points for $\eta = 0.10$, $\eta = 0.05$, and $\eta = 0.00$ (within the numerical accuracy given by the $D(R)$ oscillations which are damped more and more as η increases). If the V, Gd, or Pt dopants are introduced, the procedure becomes even more robust: Namely, further increase of the disorder increases the damping of the $D(R)$ os-
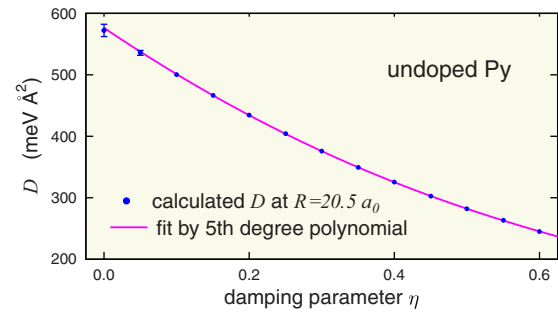

FIG. 8. Spin wave stiffness constant $D(\eta)$ for undoped Py evaluated by performing the summation in Eq. (8) up to $R_{0j}^{(\max)} = 20.5a_0$ (a_0 is the lattice constant) for several values of the damping parameter η together with the fifth-degree polynomial used to extrapolate the data to zero damping.

cillations and the values of D thus become numerically more stable.

The extrapolation is not an unambiguous procedure. One can always speculate about using a polynomial of a different degree for the fit or about varying a bit the interval of the η values for which the polynomial is fitted. Within these limits, the numerical accuracy of our values of D is a few units of meV $\mathring{A}^2$. This is sufficient for our purpose, especially given the fact that our focus is on the trends of the D values evaluated always according to the same recipe.

[1] C. A. F. Vaz, J. A. C. Bland, and G. Lauhoff, Rep. Prog. Phys. **71**, 056501 (2008).

[2] J. Kübler, *Theory of Itinerant Electron Magnetism*, International Series of Monographs on Physics (Oxford University Press, Oxford, 2000).

[3] Y. Yin, F. Pan, M. Ahlberg, M. Ranjbar, P. Dürrenfeld, A. Houshang, M. Haidar, L. Bergqvist, Y. Zhai, R. K. Dumas, A. Delin, and J. Åkerman, Phys. Rev. B **92**, 024427 (2015).

[4] F. Pan, J. Chico, J. Hellsvik, A. Delin, A. Bergman, and L. Bergqvist, Phys. Rev. B **94**, 214410 (2016).

[5] S. Lepadatu, J. S. Claydon, C. J. Kinane, T. R. Charlton, S. Langridge, A. Potenza, S. S. Dhesi, P. S. Keatley, R. J. Hicken, B. J. Hickey, and C. H. Marrows, Phys. Rev. B **81**, 020413(R) (2010).

[6] S. Lepadatu, J. S. Claydon, D. Ciudad, C. J. Kinane, S. Langridge, S. S. Dhesi, and C. H. Marrows, Appl. Phys. Lett. **97**, 072507 (2010).

[7] A. Hrabec, F. J. T. Gonçalves, C. S. Spencer, E. Arenholz, A. T. N'Diaye, R. L. Stamps, and C. H. Marrows, Phys. Rev. B **93**, 014432 (2016).

[8] A. I. Liechtenstein, M. I. Katsnelson, V. P. Antropov, and V. A. Gubanov, J. Magn. Magn. Mater. **67**, 65 (1987).

[9] M. Pajda, J. Kudrnovský, I. Turek, V. Drchal, and P. Bruno, Phys. Rev. B **64**, 174402 (2001).

[10] J. Thoene, S. Chadov, G. Fecher, C. Felser, and J. Kübler, J. Phys. D: Appl. Phys. **42**, 084013 (2009).

[11] P. Dürrenfeld, F. Gerhard, J. Chico, R. K. Dumas, M. Ranjbar, A. Bergman, L. Bergqvist, A. Delin, C. Gould, L. W. Molenkamp, and J. Åkerman, Phys. Rev. B **92**, 214424 (2015).

[12] O. N. Mryasov, U. Nowak, K. Y. Guslienko, and R. W. Chantrell, Europhys. Lett. **69**, 805 (2005).

[13] O. N. Mryasov, Phase Transitions **78**, 197 (2005).

[14] M. Ležaić, P. Mavropoulos, J. Enkovaara, G. Bihlmayer, and S. Blügel, Phys. Rev. Lett. **97**, 026404 (2006).

[15] S. Polesya, S. Mankovsky, O. Šipr, W. Meindl, C. Strunk, and H. Ebert, Phys. Rev. B **82**, 214409 (2010).

[16] J. P. Nibarger, R. Lopusnik, Z. Celinski, and T. J. Silva, Appl. Phys. Lett. **83**, 93 (2003).

[17] J. M. Shaw, H. T. Nembach, T. J. Silva, and C. T. Boone, J. Appl. Phys. **114**, 243906 (2013).

[18] H. Ebert, D. Ködderitzsch, and J. Minár, Rep. Prog. Phys. **74**, 096501 (2011).

[19] H. Ebert, *The* SPRKKR *package version 7*, http://olymp.cup.uni-muenchen.de/ak/ebert/SPRKKR (2014).

[20] J. Kudrnovský and V. Drchal, Phys. Rev. B **41**, 7515 (1990).

[21] K. Carva, J. Kudrnovský, F. Máca, V. Drchal, I. Turek, P. Baláž, V. Tkáč, V. Holý, V. Sechovský, and J. Honolka, Phys. Rev. B **93**, 214409 (2016).

[22] M. Richter, in *Handbook of Magnetic Materials*, Vol. 13, edited by K. H. J. Buschow (North-Holland, Amsterdam, 2001), pp. 87–228.

[23] I. Turek, J. Kudrnovský, G. Bihlmayer, and S. Blügel, J. Phys.: Condens. Matter **15**, 2771 (2003).

[24] J. Rusz, I. Turek, and M. Diviš, Phys. Rev. B **71**, 174408 (2005).

[25] S. Khmelevskyi, T. Khmelevska, A. V. Ruban, and P. Mohn, J. Phys.: Condens. Matter **19**, 326218 (2007).

[26] Y. Yin, M. Ahlberg, P. Dürrenfeld, Y. Zhai, R. K. Dumas, and J. Åkerman, IEEE Magn. Lett. **8**, 3502604 (2017).

[27] J. Mathon and E. P. Wohlfarth, Proc. Roy. Soc. (London) A **302**, 409 (1968).

[28] P. Riedi, Physica B+C **91**, 43 (1977).

[29] S. N. Kaul and P. D. Babu, Phys. Rev. B **50**, 9308 (1994).

[30] P. Yu, X. F. Jin, J. Kudrnovský, D. S. Wang, and P. Bruno, Phys. Rev. B **77**, 054431 (2008).

[31] I. Nakai, J. Phys. Soc. Jpn. **52**, 1781 (1983).

[32] R. Pauthenet, J. Appl. Phys. **53**, 2029 (1982).

[33] C. Loong, J. M. Carpenter, J. W. Lynn, R. A. Robinson, and H. A. Mook, J. Appl. Phys. **55**, 1895 (1984).

[34] P. W. Mitchell and D. M. Paul, Phys. Rev. B **32**, 3272 (1985).

[35] M. Hennion, B. Hennion, A. Castets, and D. Tocchetti, Solid State Commun. **17**, 899 (1975).

[36] S. A. Khan, J. Minár, H. Ebert, P. Blaha, and O. Šipr, Phys. Rev. B **95**, 014408 (2017).